PROD. TYPE: FTP
PP: 1-17 (col.fig.: nil)
CES7034 MODE+
ED: Pabitra
PAGN: Prabhu.I – SCAN: nil
ARTICLE IN PRESS
ELSEVIER
Chemical Engineering Science ▮▮▮ (▮▮▮▮) ▮▮▮–▮▮▮
Chemical Engineering Science
www.elsevier.com/locate/ces

Simulation of a multi-annular photocatalytic reactor for degradation of perchloroethylene in air
Parametric analysis of radiative energy efficiencies

Gustavo E. Imoberdorf, Alberto E. Cassano, Horacio A. Irazoqui, Orlando M. Alfano*

INTEC, Instituto de Desarrollo Tecnológico para la Industria Química (Universidad Nacional del Litoral and CONICET), Güemes 3450, S3000GLM Santa Fe, Argentina

Received 4 March 2006; received in revised form 18 October 2006; accepted 26 October 2006

Abstract

A multi-annular photocatalytic reactor was designed, that shows good effectiveness for perchloroethylene (PCE) removal from contaminated air streams. In a previous work, a rigorous physical and mathematical model of the photocatalytic reactor was developed and experimentally verified. In this work, this mathematical model was used to study the radiative energy efficiency of the multi-annular photoreactor. The total quantum efficiency is defined as the ratio of the number of molecules of PCE reacted to the number of photons emitted by the lamp, and it is expressed as the product of the following factors: the reactor radiation incidence efficiency, the catalyst radiation absorption efficiency, and the overall reaction quantum efficiency. For the employed reactor, the numerical values of each one were 83%, 92%, and $< 2.5\%$, respectively. Particularly, the dependence of the overall reaction quantum efficiency upon operating variables such as the PCE feed concentration, gas flow rate, irradiation level and relative air humidity was analyzed. These results are useful to optimize the operating conditions and design parameters of the photocatalytic reactor.
© 2006 Published by Elsevier Ltd.

Keywords: Photocatalysis; Energy efficiencies; Pollution; Remediation; Simulation; Mathematical modeling

UNCORRECTED PROOF

1. Introduction

The legislation and environmental regulations regarding the presence of undesirable volatile organic compounds (VOCs) in air are becoming more stringent than ever before. Many VOCs are chemical pollutants of air, thus posing a serious environmental threat to the public health. Photocatalysis is one among the advanced oxidation techniques that are being studied for the treatment of polluted air from different sources. The effectiveness of this process for the elimination of many air organic pollutants has been proven, as it is the case of alcohols, ketones, aromatic organics, nitrogen and halogenated compounds (Hoffman et al., 1995; Peral et al., 1997; Blake, 2001; Zhao and Yang, 2003). Its potential applications are aimed at solving contamination problems of indoor air, such as those existing in offices, residences and industrial facilities, by eliminating toxic gases and obnoxious odors (Fujishima et al., 2000).

Photocatalytic oxidation of chlorinated organic compounds, such as trichloroethylene (TCE) or perchloroethylene (PCE), deserves special attention due to the toxicity and the resistance to biodegradation of these chemicals (Hung and Mariñas, 1997; Amama et al., 2001; Wang et al., 2002; Yamazaki and Araki, 2002; Demeestere et al., 2004, Hegedüs and Dombi, 2004a,b).

In practice, the application of processes involving photoreactors are often limited by the operating costs associated with the production of photons. Consequently, in photocatalytic processes, in addition to the effort directed at obtaining high active catalysts and at identifying the best operating conditions to carry out the chemical reactions involved, it is also necessary to pay special attention to those factors of the reactor design restricting the optimal use of the radiation energy. Configurations that may be appropriate for thermal catalytic processes

* Corresponding author. Tel.: +54 342 451 1546/47; fax: +54 342 451 1087.
E-mail address: alfano@intec.unl.edu.ar (O.M. Alfano).

0009-2509/$ - see front matter © 2006 Published by Elsevier Ltd.
doi:10.1016/j.ces.2006.10.024

Please cite this article as: G.Imoberdorf, E., et al., Simulation of a multi-annular photocatalytic reactor for degradation of perchloroethylene in air. Chemical Engineering Science (2006), doi: 10.1016/j.ces.2006.10.024

cannot be extrapolated to those involving "cold" electromagnetic radiation fields. The direct adoption of packed bed reactor configurations without making allowance for the specific features of the radiation field in a photocatalytic reactor may cause that only a small fraction of the catalyst surface will be effectively irradiated and activated. Most of the catalyst surface may remain inactive in dark zones far from the lamp or in the interior of the pores. Similar considerations can be made with respect to monolithic reactors. They are widely used in thermal catalytic processes due to their very appealing surface-to-volume ratio and to the small pressure drop associated with the fluid flow. However, in photocatalytic applications the existence of large radiation flux gradients (i.e., very short radiation penetration depth inside the monolith channels) turns useless a significant fraction of the available catalytic area (Hossain and Raupp, 1999). To get round this problem, a reactor configuration has been proposed that consists of a sequence of modules, each one consisting in a set of lamps illuminating monoliths of very small depth (Raupp et al., 2001).

Since the energy consumption is one of the most significant barriers to photocatalytic applications, it is important for the designer to focus his attention on how efficiently the radiative energy is used in reactors with different configurations, or in the same reactor operating under different conditions, always fulfilling the same task. The key tool for this analysis is the reactor quantum efficiency. Different definitions have been proposed for the radiative energy efficiency of photoreactors, leading to different ways of assessing their energy performance (Cerdá et al., 1977; Serpone and Emeline, 2002; Ibrahim and de Lasa, 2003).

Although the definition of the reaction quantum yield was meant for monochromatic radiation, quantum efficiencies should be used for polychromatic radiation instead (Braun et al., 1986; Cabrera et al., 1994). A widely employed criterion is the use of the apparent quantum efficiency. In the case of the photocatalytic elimination of air pollutants, it can be defined as the ratio of the global rate of degradation of the contaminant species, to the total energy entering the photocatalytic reactor per unit time.

Few studies on the apparent quantum efficiency of the photocatalytic degradation of chlorinated organic compounds in gas phase can be found in the scientific literature. Yamazaki–Nishida et al. (1993) studied the degradation of TCE, which follows a mechanism similar to that of PCE. They obtained apparent quantum efficiencies ranging from 40% to 90%, in a fixed-bed reactor filled with porous spheres of TiO_2, which were synthesized with a sol–gel technique. The concentration of TCE, which has a great impact on the apparent quantum efficiency, was 460 ppm (approximately tenfold the PCE concentration used in this work). For the degradation of TCE, Jacoby et al. (1995) found apparent quantum efficiencies ranging from 30% to 40% for TCE concentrations around 400 ppm. In their experiments they used an annular reactor with TiO_2 immobilized on the reactor walls by means of an impregnation technique. The degradation of TCE has been also studied by Buechler et al. (1999). They used an annular/tubular reactor irradiated with eight black-light type lamps located in a circular arrangement, external to the reactor, with controlled periodic illumination. Their work was focused on the reactor performance under different rate control regimes of the overall process comprising the chemical reaction coupled with mass transfer. They determined that under kinetic control regime, the apparent quantum efficiency reached values close to 150%, with a TCE initial concentration of 80 ppm and an irradiation levels between 0.2 and 1.3 mW cm^{-2}. Ozaki et al. (2002) studied the photocatalytic degradation of gaseous mixtures of chloroethylenes in a batch reactor. They used high PCE initial concentrations (2000 ppm) and achieved remarkable apparent quantum efficiencies as high as 1060%.

Unfortunately, it is difficult to advance a diagnosis about the factors constraining the energy performance of photocatalytic reactors, or to take measures towards its improvement, on the basis of their apparent quantum efficiency only. A more conclusive analysis can be done if we assess the impact that each individual event, in the sequence starting with the emission of photons by the lamp and ending with its usage in the photocatalytic reaction, has on the total radiative energy efficiency.

Our first contribution in the series to which the present work belongs, dealt with the task of deriving an intrinsic kinetic model for the degradation of PCE based on a proposed reaction scheme, as well as with its experimental validation (Imoberdorf et al., 2005). All the experimental work was done using reactors with the TiO_2 photocatalyst immobilized on the glass walls in the form of thin films, deposited with a sol–gel technique. The developed kinetic model accounts for the effect of changes in the PCE feed concentrations, as well as in the relative humidity and irradiation level. The intrinsic kinetic expression for PCE degradation was validated in a titanium dioxide coated plate photoreactor operated under kinetic control regime, free of mass transfer interferences. Afterwards, this kinetic expression became a key item in the physical modeling and mathematical simulation of a multi-annular, bench-scale reactor (Imoberdorf et al., 2006). The photocatalytic reactor having a multi-annular configuration showed good effectiveness for the PCE degradation in polluted, moist air. A model of the radiation field was developed to predict the local superficial rate of photon absorption (LSRPA) at each point on the reactor catalytic walls, which is needed to evaluate the local reaction rate. A two-dimensional differential mass balance model was proposed, which included mass transfer rate processes in the gas phase, as well as the intrinsic PCE degradation kinetics appearing in the boundary conditions at the reactor walls. The differential mass balance equation for PCE was coupled to the LSRPA calculated with the radiation field model equations through the included degradation kinetics. Predicted conversions agreed with experimental results within a root mean square error smaller than 5.6%.

In this work, the analysis of the radiative energy efficiency of the multi-annular photocatalytic reactor for PCE degradation will be carried out in a way that accounts for the impact on the total radiative energy efficiency, of each event in the succession starting with the initial emission of photons by the lamp and ending with its final usage in the catalytic degradation reaction. Particularly, the dependence of the overall reaction quantum efficiency for PCE degradation upon operating variables such

UNCORRECTED PROOF

Please cite this article as: G.Imoberdorf, E., et al., Simulation of a multi-annular photocatalytic reactor for degradation of perchloroethylene in air. Chemical Engineering Science (2006), doi: 10.1016/j.ces.2006.10.024

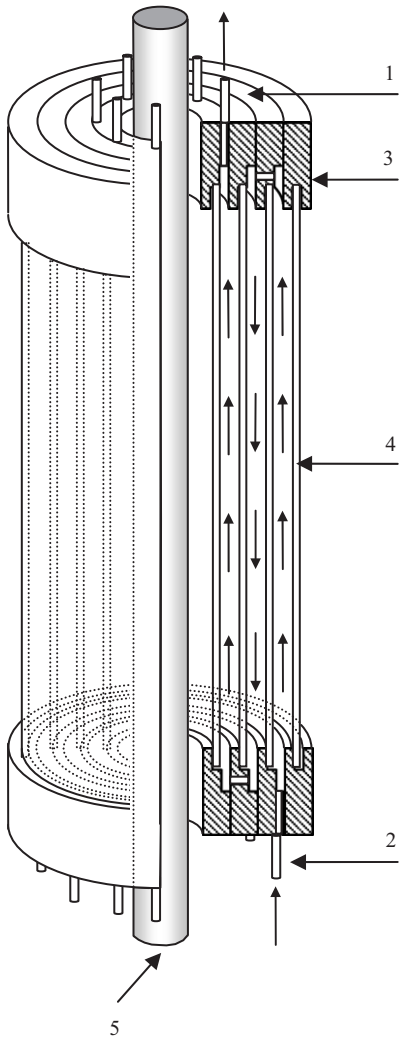

Fig. 1. Geometry of the multi-annular photocatalytic reactor. Keys: (1) gas outlet; (2) gas inlet; (3) distribution head; (4) borosilicate glass tubes; (5) UV lamp.

as the PCE feed concentration, gas flow rate, irradiation level and relative air humidity is studied. For this, the simulation program comprising the mass transfer, the radiation field and the degradation kinetic models, experimentally validated in our previous work, will be used.

2. Experimental section

The reactor consists of four concentric cylindrical, borosilicate glass tubes (Fig. 1) which are transparent to UVA radiation in most of the useful wavelength range (from 300 to 420 nm). A tubular UV lamp (Philips TL 18W/08 F4T5/BLB) was placed at the central axis of the system. Reactants and products flowed trough the annular spaces, entering the reactor by the external annular space and leaving it by the internal one. The two walls directly in contact with the gas flowing through each annulus were covered with a thin layer of TiO_2. The inner and the outer tubes were covered only on the side in contact with the contaminated air stream. The very thin layers of TiO_2 were deposited using a sol–gel technique (Imoberdorf et al., 2005). The reactor dimensions are reported in Table 1. One of the design parameters improving the reactor efficiency is the reduction of the annular channels widths, because smaller annular channel widths tend to reduce the reactants diffusive resistances. This was one of the aspects that received much attention in the stage of the multi-annular reactor design. Among the borosilicate glass tubes available in the market we chose those that could be combined in a way that they give rise to an arrangement of annular channels with the smaller possible widths. With more choices in the market of good quality borosilicate tubes, further arrangement of channels could be analyzed.

Experimental data were gathered using a bench-scale setup schematically shown in Fig. 2. The photoreactor feed stream results from mixing a dry air stream with a water-saturated air stream obtained by bubbling dry air in a saturation flask containing distilled water at 20 °C, and a dry air stream with PCE, in different proportions so that the desired PCE feed concentration and relative humidity for each run could be obtained. With this setup, the flow rate of the feed stream can be easily controlled as well. Chromatographic quality air (air liquid) and liquid PCE (Merck, p.a. quality) were used to prepare the moist PCE-air feed mixture. The flow rates of the three streams before being mixed were controlled with on-line mass-flow controllers (Matheson Corp.). The temperature and the humidity of the feed stream were measured with an on-line thermohygrometer (Oakton 35612-00) located just upstream from the sampling point in the reactor feed line.

Before starting each experimental run, the operating variables were fixed at the pre-established values and then the lamp was turned on. Samples were taken from the two sampling points not before 3 h of continuous operation to ensure a steady state regime of the reaction system and a constant light intensity. The PCE concentrations in the inlet and outlet streams were determined by off-line gas chromatography (Hewlett Packard 5890; J&W1257032 column; FID detector). The spectral radiation absorption of the photocatalytic tubes and filters employed to modulate the irradiation rates, were measured with a UV–Vis spectrophotometer (Varian Cary, 100 Bio) as a function of wavelength, within the emission range of the lamp.

3. Model development

3.1. Flow model and mass balances

We will make the following assumptions for the reactor operating in steady state: (i) the gas flow through each of the annular ducts is a unidirectional, incompressible and fully developed laminar flow along the entire useful reactor length, thus disregarding the relative importance of end effects; (ii) the contaminated moist air stream behaves as a Newtonian fluid; (iii) due to the reactor configuration, every scalar field (for instance, the PCE concentration field) remains invariant under virtual solid rotations about de lamp axis (azimuthal symmetry), thus reducing both the physical and the mathematical descriptions to two-dimensional problems; (iv) constant and uniform tempera-

UNCORRECTED PROOF

Please cite this article as: G.Imoberdorf, E., et al., Simulation of a multi-annular photocatalytic reactor for degradation of perchloroethylene in air. Chemical Engineering Science (2006), doi: 10.1016/j.ces.2006.10.024

Table 1
Reactor dimensions and experimental operating conditions

Description		Values	Units
Lamp	Length	59	cm
	Radius	1.4	cm
	Output power	3.5	W
Reactor	Length	48	cm
	Radius	4.26	cm
	Reactive surface	5205	cm^2
	Inner radius 1	1.69	cm
	Outer radius 1	2.31	cm
	Inner radius 2	2.51	cm
	Outer radius 2	3.30	cm
	Inner radius 3	3.53	cm
	Outer radius 3	3.94	cm
Feed flow rate		2–30	$cm^3\,s^{-1}$
Temperature		20	°C
Pressure		101325	Pa
Inlet PCE concentration		5–50	$mg\,m^{-3}$
Relative humidity		10–90	%
SRPA		1.0×10^{-11}–2×10^{-9}	Einstein $cm^{-2}\,s^{-1}$

ture field; and (v) constant physical parameters (e.g., viscosity, density). The coordinate system for the reactor model is shown in Fig. 3a. The fully developed velocity profile for a laminar flow of a Newtonian fluid through the jth annular duct is

$$V_{z,j}(r) = (-1)^{j+1}\frac{2Q}{\pi R_j^2}\frac{\ln\chi_j}{[(1-\chi_j^4)\ln\chi_j + (1-\chi_j^2)^2]} \times\left[1-\left(\frac{r}{R_j}\right)^2 - \frac{(1-\chi_j^2)}{\ln\chi_j}\ln\left(\frac{r}{R_j}\right)\right] \quad (j=1,2,3), \tag{1}$$

where the upward direction was chosen as the positive one.

The differential mass balance equation will be simplified on the basis of the following considerations: (vi) negligible contribution of the molecular diffusion mechanism to the total axial mass flow density when compared with the convective contribution. Thus, the axial mass flow is considered essentially convective, remaining the diffusive flux important only along the radial direction. (vii) Because the concentration of the more abundant species in the flowing reactant stream as well as its temperature are constant in the reactor, the diffusivities of the species in the gas mixture are assumed constant. Although always dilute, PCE is the only species that changes its concentration along the reactor in measurable quantities. Therefore, the radial diffusion can be approximated as that of PCE in air. This will be the governing mass transfer mechanism of PCE from the bulk of the gas stream to the catalytic boundaries. (viii) Chemical reactions only take place on the photocatalytic film deposited on the annular walls in contact with the flowing contaminated air stream or in its immediate vicinity. True homogeneous photochemical reactions are considered completely absent, an expected result from the absorption spectrum of PCE in the employed wavelength interval. (ix) The internal diffusive resistance has been considered negligible due to the low thickness of the TiO_2 films (the estimated value is lower than 200 nm), and due to the high PCE-air diffusivity. With assumptions (i)–(ix), the differential mass transfer equation can be written as

$$\frac{\partial C_{PCE}(r,z)}{\partial z}V_{z,j}(r) = \frac{D^0_{PCE\text{-}Air}}{r}\frac{\partial}{\partial r}\left(r\frac{\partial C_{PCE}(r,z)}{\partial r}\right) \quad (0<z<Z_R;\ \chi_j R_j<r<R_j;\ j=1,2,3) \tag{2}$$

with the boundary conditions

$$D^0_{PCE\text{-}Air}\left.\frac{\partial C_{PCE}(r,z)}{\partial r}\right|_{r=R_j} = r_{PCE}(R_j,z) \quad (0<z<Z_R;\ j=1,2,3), \tag{3}$$

$$D^0_{PCE\text{-}Air}\left.\frac{\partial C_{PCE}(r,z)}{\partial r}\right|_{r=\chi_j R_j} = -r_{PCE}(\chi_j R_j,z) \quad (0<z<Z_R;\ j=1,2,3), \tag{4}$$

where C_{PCE} is the PCE concentration, $D^0_{PCE\text{-}Air}$ is the diffusion coefficient of PCE in air ($D^0_{PCE\text{-}Air} = 0.072\,cm^2\,s^{-1}$), and r_{PCE} is the PCE reaction rate on the catalytic surface. The PCE concentration at the inlet of an annular section can be obtained from the corresponding expression among those given by

$$C_{PCE}(r,z)|_{z=0} = C^{in}_{PCE} \quad (\chi_3 R_3 < r < R_3), \tag{5}$$

$$C_{PCE}(r,z)|_{z=Z_R} = \frac{\int_{k_3R_3}^{R_3} C_{PCE}(r,Z_R)V_{z,3}(r)r\,dr}{\int_{k_3R_3}^{R_3} V_{z,3}(r)r\,dr} \quad (\chi_2 R_2 < r < R_2), \tag{6}$$

$$C_{PCE}(r,z)|_{z=0} = \frac{\int_{k_2R_2}^{R_2} C_{PCE}(r,0)V_{z,2}(r)r\,dr}{\int_{k_2R_2}^{R_2} V_{z,2}(r)r\,dr} \quad (\chi_1 R_1 < r < R_1). \tag{7}$$

UNCORRECTED PROOF

Please cite this article as: G.Imoberdorf, E., et al., Simulation of a multi-annular photocatalytic reactor for degradation of perchloroethylene in air. Chemical Engineering Science (2006), doi: 10.1016/j.ces.2006.10.024

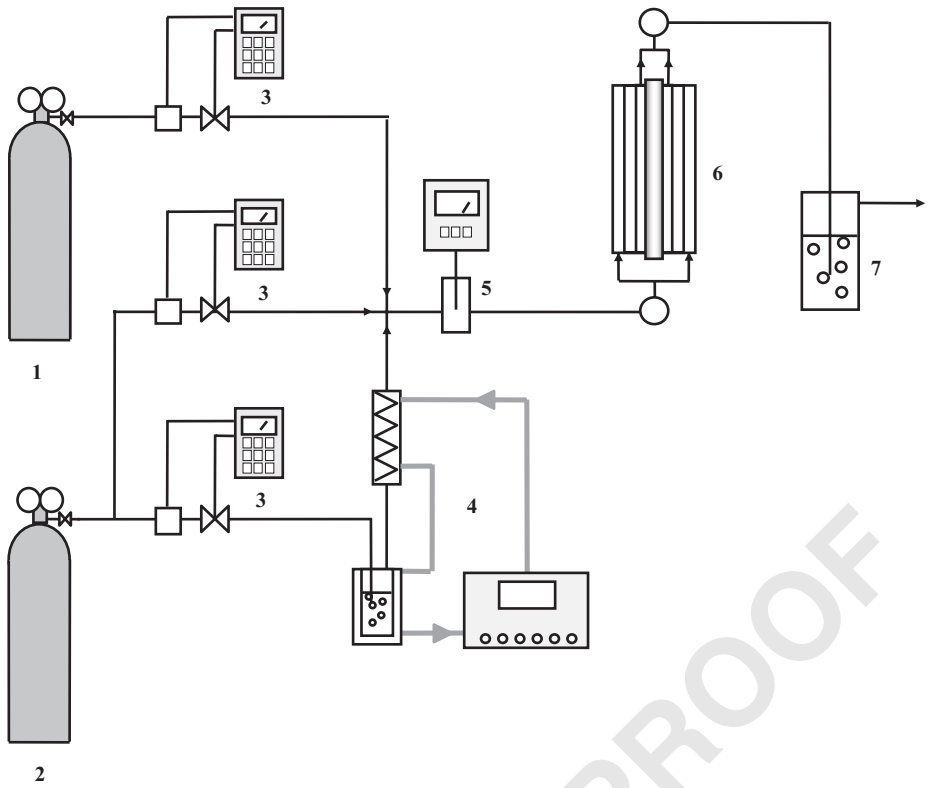

Fig. 2. Flow sheet of the experimental device: (1) PCE + air; (2) air; (3) mass flowmeters; (4) humidifier system (saturation flask, heat exchanger and thermostatic bath); (5) thermohygrometer; (6) photoreactor with inlet and outlet sampling devices; (7) gas scrubber.

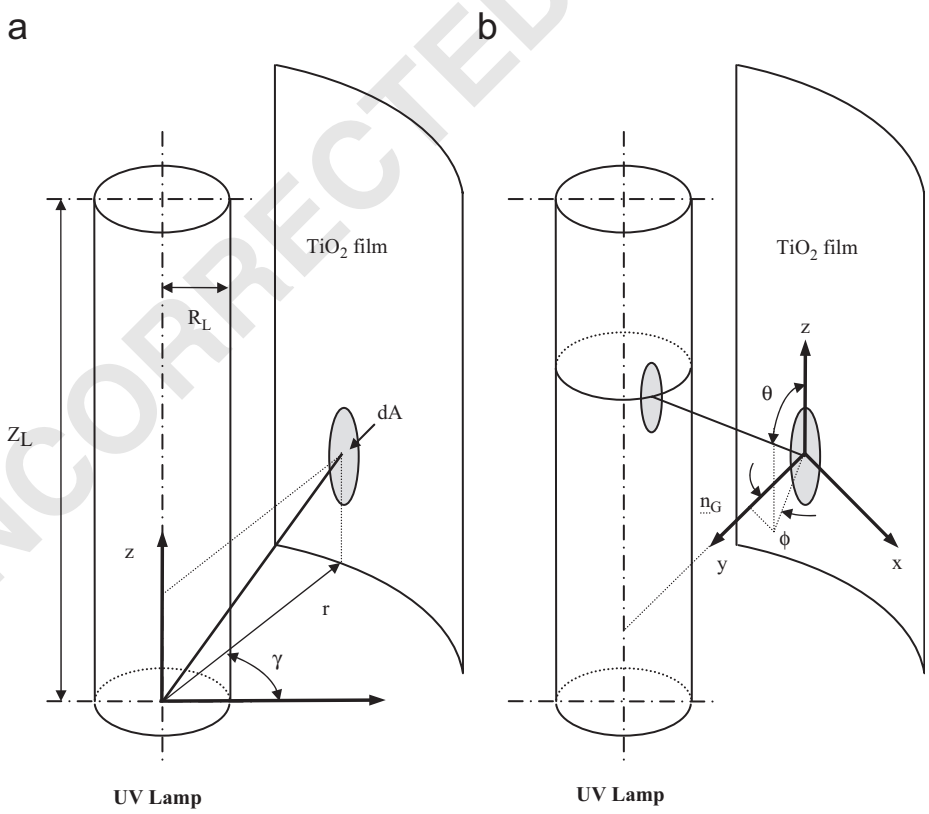

Fig. 3. (a) Cylindrical coordinate system for the reactor model; (b) spherical coordinate system for the radiation model.

UNCORRECTED PROOF

Please cite this article as: G.Imoberdorf, E., et al., Simulation of a multi-annular photocatalytic reactor for degradation of perchloroethylene in air. Chemical Engineering Science (2006), doi: 10.1016/j.ces.2006.10.024

The PCE average concentration at the reactor outlet is computed as follows:

$$C_{\mathrm{PCE}}^{\mathrm{out}} = \frac{\int_{\chi_1 R_1}^{R_1} C_{\mathrm{PCE}}(r, Z_R) V_{z,1}(r) r \, \mathrm{d}r}{\int_{\chi_1 R_1}^{R_1} V_{z,1}(r) r \, \mathrm{d}r}. \tag{8}$$

3.2. Kinetic model

The surface rate of the PCE elimination reaction (r_{PCE}) is part of the expression of the boundary conditions of Eqs. (3) and (4). In our earlier work (Imoberdorf et al., 2005), an expression of the intrinsic reaction rate was derived from a reaction scheme. This mechanism was based on that proposed by Sanhueza et al. (1976) for TCE degradation in gas phase. Although there is no full agreement on it, this reaction scheme was accepted by many authors (Li and An, 2000; Amama et al., 2001; Zhao et al., 2002; Yamazaki et al., 2004; Tanimura et al., 2005). Moreover, Yamazaki et al. (2001) and Yamazaki and Araki (2002) proposed a similar mechanism for the PCE degradation reaction.

In a previous work, an expression of the intrinsic kinetics for the degradation of PCE based on a plausible reaction mechanism was proposed (Imoberdorf et al., 2005). The expression of the PCE degradation rate was

$$r_{\mathrm{PCE}} = -\frac{k' C_{\mathrm{PCE}} C_{\mathrm{H_2O}}}{(1 + K_{\mathrm{PCE}} C_{\mathrm{PCE}} + K_{\mathrm{H_2O}} C_{\mathrm{H_2O}})^2} \times \left(-1 + \sqrt{k'' \frac{1 + K_{\mathrm{PCE}} C_{\mathrm{PCE}} + K_{\mathrm{H_2O}} C_{\mathrm{H_2O}}}{C_{\mathrm{H_2O}}} e^{a,s} + 1} \right), \tag{9}$$

where $e^{a,s}$ is the number of photons absorbed on the catalytic surface per unit time and unit area or the local surface rate of photon absorption (LSRPA); K_{PCE} and $K_{\mathrm{H_2O}}$ are the adsorption equilibrium constants of PCE and water on the TiO_2 catalyst film, respectively; and k' and k'' are kinetic parameters.

The degradation of PCE from a moist air stream was studied for different values of PCE feed concentrations, relative humidities, and irradiation levels in a flat-plate reactor without mass transfer limitations (Imoberdorf et al., 2005). For the experimental conditions used, it was shown that Eq. (9) can be simplified to give

$$r_{\mathrm{PCE}} = -\alpha \frac{C_{\mathrm{PCE}}}{1 + K_{\mathrm{H_2O}} C_{\mathrm{H_2O}}} e^{a,s}. \tag{10}$$

The parameters in the reaction rate expression of Eq. (10) were regressed from experimental data using the Levenberg–Marquardt method, the resulting values being $\alpha = (1.54 \pm 0.19) \times 10^8$ ($\mathrm{cm^3\,Einstein^{-1}}$) and $K_{\mathrm{H_2O}} = (3.21 \pm 0.51) \times 10^{-4}$ ($\mathrm{m^3\,mg^{-1}}$).

3.3. The radiation field and the local surface rate of energy absorption

For the numerical evaluation of expression (10), it is necessary to knowing the value of LSRPA at every point on the photocatalytic surface of the multi-annular reactor. These values are not amenable to experimental measurement and therefore, they had to be computed from the radiation field model described below.

The LSRPA was calculated at each point on the TiO_2 films, taking into account the radiation incident from all feasible directions. The spectral net radiation flux q_λ, with the adopted coordinate system (Fig. 3b), is given by

$$q_\lambda(r, z) = \int_\phi \int_\theta I_\lambda(r, z, \phi, \theta) \cos\phi \sin^2\theta \, \mathrm{d}\theta \, \mathrm{d}\phi, \tag{11}$$

where I_λ is the intensity of an energy beam of wavelength λ which travels in the (θ, ϕ) direction at the (r, z) position. In order to compute $q_\lambda(r, z)$ from Eq. (11) we will adopt the three-dimensional source with superficial emission model (Cassano et al., 1995) and a ray-tracing computational method. The radiation beams coming directly from the lamp, which are incident on a differential area at a position (r, z) on the catalytic film, can only have directions within the limits defined by the lamp contour as seen from the point of incidence. In terms of the (θ, ϕ) spherical coordinates, this contour is the solution of the following set of equations:

$$\phi_{\max}(r) = \cos^{-1}\left(\frac{\sqrt{r^2 - R_L^2}}{r}\right), \quad \phi_{\min}(r) = -\cos^{-1}\left(\frac{\sqrt{r^2 - R_L^2}}{r}\right), \tag{12}$$

$$\theta_{\max}(r, z, \phi) = \tan^{-1}\frac{r\cos\phi - \sqrt{R_L^2 - r^2\sin\phi^2}}{z}, \quad \theta_{\min}(r, z, \phi) = \tan^{-1}\frac{r\cos\phi - \sqrt{R_L^2 - r^2\sin\phi^2}}{Z_L - z}. \tag{13}$$

From the lamp model adopted, the following boundary condition for the light intensity results:

$$I_{\lambda,L}(r, z, \phi, \theta) = I_{\lambda,L} = \frac{P_{\lambda,L}}{2\pi^2 R_L Z_L}, \tag{14}$$

where $P_{\lambda,L}$ is the spectral emission power of the lamp, and R_L and Z_L are the radius and length of the lamp, respectively. The value of $P_{\lambda,L}$ may be obtained from the lamp manufacturer. Substitution of Eqs. (12)–(14) in Eq. (11) and evaluating on the inner radius of the reactor ($R_{R,\mathrm{int}}$), we obtain the spectral net radiation flux on the reactor wall of radiation entrance ($q_{\lambda,RW}$):

$$Q_{\lambda,RW} = \int_{\phi_{\min}(R_{R,int})}^{\phi_{\max}(R_{R,int})} \int_{\theta_{\min}(R_{R,\mathrm{pint}},z,\phi)}^{\theta_{\max}(R_{R,\mathrm{int}},z,\phi)} I_{\lambda,L} \cos\phi \sin^2\theta \, \mathrm{d}\theta \, \mathrm{d}\phi. \tag{15}$$

At every position on the thin catalytic film, the LSRPA can be obtained from the local net radiation fluxes resulting from all incident radiation beams coming from the lamp

$$e_\lambda^{a,s}(r, z) = q_\lambda^i(r, z) - q_\lambda^t(r, z), \tag{16}$$

UNCORRECTED PROOF

Please cite this article as: G.Imoberdorf, E., et al., Simulation of a multi-annular photocatalytic reactor for degradation of perchloroethylene in air. Chemical Engineering Science (2006), doi: 10.1016/j.ces.2006.10.024

where $q^i_\lambda(r,z)$ and $q^t_\lambda(r,z)$ are the incident and transmitted net radiation fluxes, respectively. It should be noticed that Eq. (16) results from a balance of radiant energy, with the assumption that the photocatalytic film thickness are very thin in comparison with its distance to the radiation source. Substitution of Eqs. (11)–(15) in Eq. (16), and considering the attenuation produced by each participative medium along the path of the radiation beams, the final expression of the LSRPA at a given position on a catalytic film is (Imoberdorf et al., 2006):

$$e^{a,s}(r,z)=\sum_{\lambda=300\,\mathrm{nm}}^{420\,\mathrm{nm}}\int_{\phi_{\min}(r)}^{\phi_{\max}(r)}\int_{\theta_{\min}(r,z,\phi)}^{\theta_{\max}(r,z,\phi)} I_{\lambda,L}\exp \times\left(-n_g(r)\frac{\kappa_{\lambda,g}e_g}{\cos\alpha_n}-n_f(r)\frac{\kappa_{\lambda,f}e_f}{\cos\alpha_n}\right) \times\left[1-\exp\left(-\frac{\kappa_{\lambda,f}e_f}{\cos\alpha_n}\right)\right]\cos\phi\sin^2\theta\,\mathrm{d}\theta\,\mathrm{d}\phi, \quad (17)$$

where $\kappa_{\lambda,f}$ and $\kappa_{\lambda,g}$ are the spectral absorption coefficients of the TiO_2 film and the glass tubes, respectively; e_f and e_g are their corresponding thicknesses; α_n is the angle between the ray trajectory and the film outwardly directed normal; and n_g and n_f are the number of times that a radiation beam has been attenuated by a glass tube wall or by a TiO_2 film, respectively, before its incidence at the (r,z) position on the catalytic surface. Values of the products $\kappa_{\lambda,f}e_f$ and $\kappa_{\lambda,g}\,e_g$ were determined from spectral transmittance measurements (Imoberdorf et al., 2005).

The mean value of the LSRPA on the reactor catalytic surface is the surface rate of photon absorption (SRPA), defined as follows:

$$\langle e^{a,s}\rangle_{A_R}=\frac{\int_{A_R}e^{a,s}(r,z)\,\mathrm{d}A}{A_R}, \quad (18)$$

where A_R is the total photocatalytic surface area of the reactor. Considering all possible contributions to the value of the SRPA, Eq. (18) may be written as

$$\langle e^{a,s}\rangle_{A_R}=\frac{\sum_{j=1}^{3}\int_{z=0}^{Z_R}[\chi_j R_j e^{a,s}(\chi_j R_j,z)+R_j e^{a,s}(R_j,z)]\,\mathrm{d}z}{Z_R\sum_{j=1}^{3}(\chi_j R_j+R_j)}, \quad (19)$$

where Z_R is the reactor length and $\chi_j R_j$ and R_j are the inner and outer radius of the jth annular duct, respectively, with $j=1,2,3$ when numbered from the inner to the outer one.

4. Radiative energy efficiencies definitions

4.1. Total quantum efficiency

The total quantum efficiency (η_T) is defined as the ratio of the number of molecules of PCE decomposed to the number of photons emitted by the lamp. The efficiency η_T is a useful tool to compare the energy performance of different types of photocatalytic reactors fulfilling the same task (for instance, depleting the PCE concentration from the same inlet value to the same outlet value, with a given flow rate), or the performance of the same reactor under different operating conditions, provided that the objective pursued has been met in all cases. To facilitate reaching a diagnosis about the factors constraining the energy performance of photocatalytic reactors, or to take the proper actions towards its improvement, it is quite helpful to be able to assess the impact on η_T of the different events to which photons are subjected from their emission to their effective usage in the photocatalytic reaction.

The total process bridging the emission of photons with their final utilization in the chemical reaction, which is implied in the definition of η_T, can be separated into a succession of events, each one with its own efficiency. These events can be described as follows: (a) All the photons emitted by the lamp during a time interval, may or may not enter the reactor. The event of interest here is that photons enter the reactor. Clearly, the efficiency η_I of this event is the fraction of the photons emitted by the lamp during a time interval that enter the reactor during the same interval. We will call η_I the reactor radiation incidence efficiency. (b) The photons that entered the reactor during a time interval may or may not be absorbed by the catalyst films. The event of interest is that photons be absorbed by the photocatalyst. The efficiency η_A of this event is the fraction of the photons that having entered the reactor during a time interval, are absorbed by the catalyst during the same interval. We will call η_A the catalyst radiation absorption efficiency; and (c) Only a fraction of those photons that were absorbed by the catalyst during a time interval, is effectively used in the photocatalytic degradation of the contaminant during the same interval. The efficiency η_R of this event is the number of molecules of PCE decomposed divided by the number of photons that having been absorbed by the catalyst; η_R is called the overall reaction quantum efficiency.

The total quantum efficiency can be expressed as the product of these partial efficiencies

$$\eta_T=\eta_I\eta_A\eta_R. \quad (20)$$

The proposed expression of η_T makes it possible to assess the impact of different factors on the reactor energy performance. It offers a framework for the reaction engineer to put forward a diagnosis about the factors affecting the reactor energy usage, thus enabling him to systematically improve his designs or to choose optimal operating conditions.

4.2. Radiation incidence efficiency

The value of η_I depends on the external reactor configuration and dimensions as well as on the optical properties of its building materials. It also depends on the particular design of the source of photons and on its complementary optical devices like, for instance, a reflecting system to redirect photons towards the reaction surfaces. The efficiency η_I may be obtained as follows:

$$\eta_I=\frac{\int_{A_{RW}}\int_{\lambda_L}q_{\lambda,RW}\,\mathrm{d}\lambda\,\mathrm{d}A}{\int_{\lambda_L}P_{\lambda,L}\,\mathrm{d}\lambda}, \quad (21)$$

UNCORRECTED PROOF

Please cite this article as: G.Imoberdorf, E., et al., Simulation of a multi-annular photocatalytic reactor for degradation of perchloroethylene in air. Chemical Engineering Science (2006), doi: 10.1016/j.ces.2006.10.024

where A_{RW} is the area of radiation entrance and $q_{\lambda,RW}$ is the spectral radiative flux on the area of the reactor wall of radiation entrance. The value of $q_{\lambda,RW}$ may be obtained from the photon balance equation, or resorting to experimental techniques (radiometers, actinometers, etc.).

4.3. Radiation absorption efficiency

The catalyst radiation absorption efficiency (η_A) depends on the internal reactor configuration and on the optical properties of its building materials. The optical properties of the catalyst have the largest impact on η_A, particularly if the fluid is transparent to the employed radiation. In some cases the catalyst may absorb almost all the radiation that has entered the reactor, but this is not a frequent situation due to reflections and, in some designs, scattering. In reactors like ours, where the catalyst is immobilized on the reactor internal walls, radiation is only partially absorbed by the thin catalytic films; the rest is transmitted through the film, reflected on its surface, or absorbed by the borosilicate glass tubes. The efficiency η_A is also a function of the radiation wavelength, since the optical properties of the catalyst (absorption and reflection coefficients) show strong spectral dependence. As a consequence of this, we will have different values of η_A for the same reactor and the same catalyst depending, for example, on whether a black light, an actinic type or a medium or high pressure Mercury lamp is used as the light source. In most cases, the value of the η_A is determined by numerical computations based on a supporting radiation field model

$$\eta_A = \frac{\int_{A_R}\int_{\lambda_{\text{Lamp}}} e_\lambda^{a,s}\,\mathrm{d}\lambda\,\mathrm{d}A}{\int_{A_{RW}}\int_{\lambda_{\text{Lamp}}} q_{\lambda,RW}\,\mathrm{d}\lambda\,\mathrm{d}A}. \tag{22}$$

At this point it is important to remark that both η_I and η_A are parameters related to the inherent qualities of the reactor configuration, depending neither on the reaction taking place, nor on the chosen operating conditions (like, for instance, the flow rate of contaminated air at the reactor feed point, or the PCE concentration, as long as it is not participative in the useful region of the lamp emission spectrum).

4.4. Overall and local reaction quantum efficiency

The value of overall reaction quantum efficiency (η_R) depends on the specific reaction taking place as well as on the used photocatalyst, and is strongly affected by the reactor operating conditions. It is interesting noticing that, in the case of chain reactions, η_R can be much larger than 100%, given the fact that those reactions are propagated by intermediate species that are consumed as reactants and then regenerated as products in successive reaction steps. Another important feature of this parameter is that it must not depend on the photoreactor type or configuration. The overall reaction quantum efficiency can be defined as

$$\eta_R = -\frac{\langle r_{\text{PCE}}(r,z)\rangle_{A_R}}{\langle e^{a,s}(r,z)\rangle_{A_R}}. \tag{23}$$

By writing the numerator of Eq. (23) in terms of model predicted variables, the final expression of η_R, is

$$\eta_R = \frac{Q X_{\text{PCE}} C_{\text{PCE}}^{\text{in}}}{\langle e^{a,s}\rangle_{A_R} A_R}. \tag{24}$$

The concept of η_R can be also applied locally. Accordingly, the local reaction quantum efficiency results

$$\eta_{R,\text{loc}}(r,z) = -\frac{r_{\text{PCE}}(r,z)}{e^{a,s}(r,z)}. \tag{25}$$

In agreement with our reaction kinetic model, substitution of Eq. (10) in Eq. (25) gives

$$\eta_{R,\text{loc}}(r,z) = \alpha\frac{C_{\text{PCE}}(r,z)}{1 + K_{\text{H}_2\text{O}}\,C_{\text{H}_2\text{O}}}. \tag{26}$$

According to Eq. (26), which in turn has been derived from the kinetic model (Eq. (10)), $\eta_{R,\text{loc}}$ is proportional to the local PCE concentration on the catalytic film. From the same equation it can be concluded that, for kinetic laws depending linearly on $e^{a,s}$, $\eta_{R,\text{loc}}$ is independent of the LSRPA, and that it decreases as the relative humidity increases. The maximum value of $\eta_{R,\text{loc}}$ is found at the reactor inlet and it decreases as we follow the gas path through the reactor. This is so because the PCE concentration on the photocatalytic film decreases due to the combined effect of mass transfer limitations and larger PCE conversions.

4.5. Apparent quantum efficiency

As said before, the apparent quantum efficiency (η_{app}) has been widely adopted as a means of assessing the energy performance of photocatalytic reactors. It is expressed as the ratio of the global rate of degradation of the contaminant species, to the total energy entering the photocatalytic reactor per unit time. In our notation is equivalent to the product

$$\eta_{\text{app}} = \eta_A \eta_R. \tag{27}$$

To calculate η_{app}, the overall rate of the reaction taking place in the photocatalytic reactor and the rate of entrance of photons to the reactor is all what is needed. Although these parameters can be easily evaluated, the result gives no indication of the fraction of photons emitted by the lamp that actually enters de reactor, thus leaving aside an important aspect affecting the energy performance of different reactors.

4.6. Reference overall reaction quantum efficiency

In order to quantify the effect of mass transfer limitations on η_R, we define the reference overall reaction quantum efficiency ($\eta_{R,\text{ref}}$). This parameter represents the maximum value of η_R, only attainable if no mass transfer limitations existed in the reactor (i.e., the reactor is operated under kinetic control regime). To evaluate this efficiency, the assumption is made that there is no appreciable PCE radial concentration gradients in any of the three annular spaces. Therefore, from the mass transfer

UNCORRECTED PROOF

Please cite this article as: G.Imoberdorf, E., et al., Simulation of a multi-annular photocatalytic reactor for degradation of perchloroethylene in air. Chemical Engineering Science (2006), doi: 10.1016/j.ces.2006.10.024

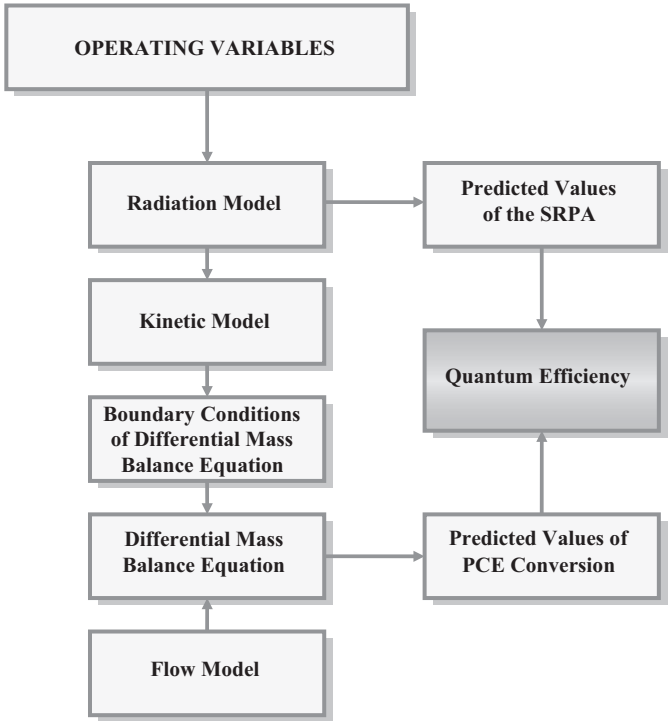

Fig. 4. Algorithm used to solve numerically the mathematical model.

differential equation (Eq. (2)) and from the boundary conditions (Eqs. (3) to (7)), we obtain (see Appendix A):

$$X_{\mathrm{PCE,ref}} = 1 - \exp\left(-\frac{\alpha A_R \langle e^{a,s}\rangle_{A_R}}{Q(1 + K_{\mathrm{H_2O}} C_{\mathrm{H_2O}})}\right). \tag{28}$$

Substitution of Eq. (28) in Eq. (24) gives

$$\eta_{R,\mathrm{ref}} = \frac{Q C^{\mathrm{in}}_{\mathrm{PCE}}}{\langle e^{a,s}\rangle_{A_R} A_R}\left(1 - \exp\left(-\frac{\alpha A_R \langle e^{a,s}\rangle_{A_R}}{Q(1 + K_{\mathrm{H_2O}} C_{\mathrm{H_2O}})}\right)\right). \tag{29}$$

Eq. (29) gives the reference overall reaction quantum efficiency as a function of the volumetric flow rate. This equation may be expressed in terms of PCE conversion, as follows:

$$\eta_{R,\mathrm{ref}} = -\frac{X_{\mathrm{PCE}} C^{\mathrm{in}}_{\mathrm{PCE}} \alpha}{\ln(1 - X_{\mathrm{PCE}})(1 + K_{\mathrm{H_2O}} C_{\mathrm{H_2O}})}. \tag{30}$$

Note that $\eta_{R,\mathrm{ref}}$ is an upper bound for the η_R, and a target only reachable under kinetic control regime, without detectable concentration gradients in the radial direction. That is why in the next section, values of η_R corresponding to different operating conditions will be compared with this reference value as a way of quantifying the impact of mass transfer on the PCE conversion and on the reactor energy performance.

5. Numerical solution and experimental validation of the mathematical model

The complete mathematical model was numerically solved with an ad hoc developed FORTRAN program, based on the solution algorithm schematically shown in Fig. 4.

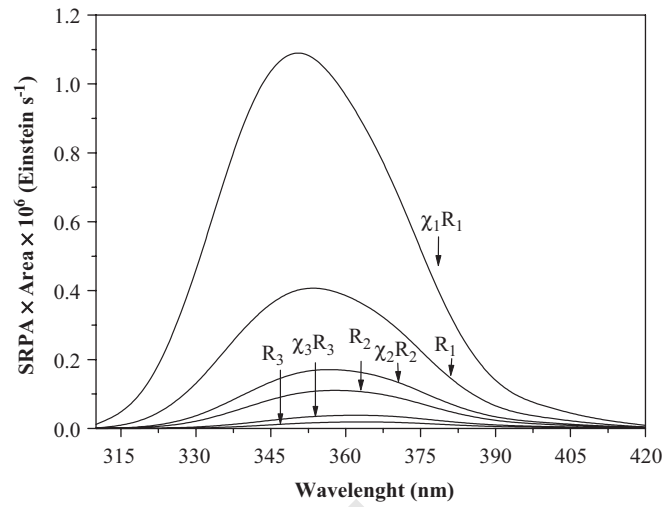

Fig. 5. Numerical values of the spectral SRPA, without neutral filters.

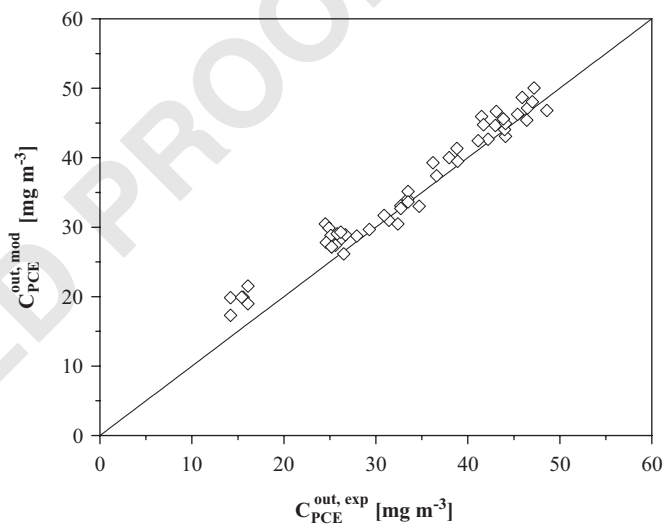

Fig. 6. Output PCE concentration for different operating conditions. Experimental values against model predictions.

The LSRPA (Eq. (17)) was computed at every point on each of the catalytic surfaces. The LSRPA depends on the physical characteristics and optical properties of different reactor components and neutral filters, if any were used. Nonetheless, the LSRPA does not depend on the PCE concentration. This is so because PCE does not absorb UV radiation in the wavelength range employed in this work. For this reason the photon balance equation is not coupled with the mass transfer equation and therefore, it can be conveniently solved as a first step in the computational scheme. The numerical results of the spectral SRPA (see Eq. (19)) are shown in Fig. 5. From these results, we conclude that the attenuation of radiation across each catalytic film is of primary importance. It should be also noticed the spectral displacement of the maximum SRPA in each TiO_2 film. This is the consequence of the wavelength dependent light absorption by the catalytic films.

UNCORRECTED PROOF

Please cite this article as: G.Imoberdorf, E., et al., Simulation of a multi-annular photocatalytic reactor for degradation of perchloroethylene in air. Chemical Engineering Science (2006), doi: 10.1016/j.ces.2006.10.024

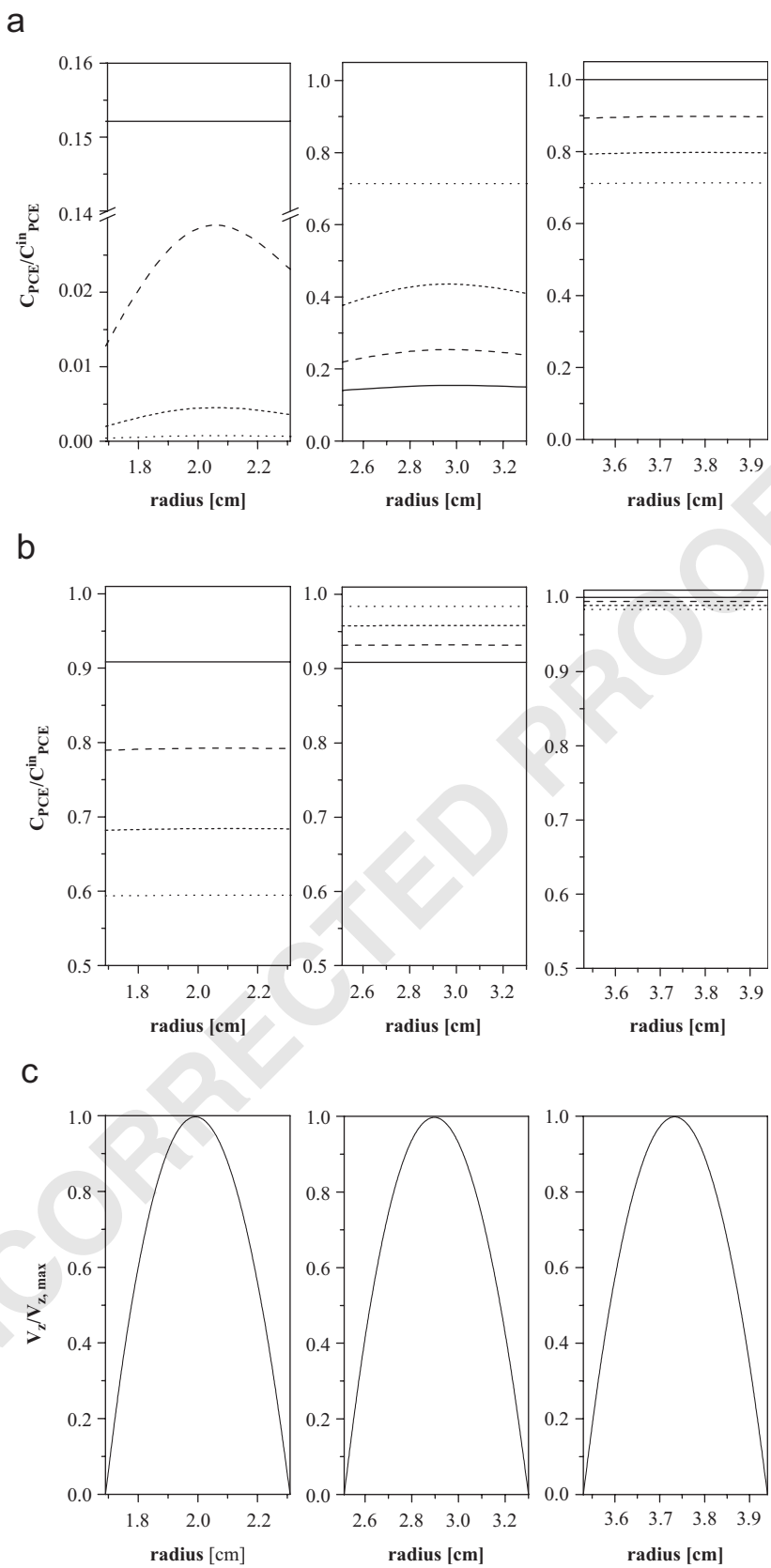

Fig. 7. Dimensionless PCE concentration radial profiles modeled for the following conditions: (a) volumetric flow rate = 30 cm^3 s^{-1}, C^{in}_{PCE} = 50 mg m^{-3}, relative humidity = 48%, SRPA = 1.56×10^{-9} Einstein cm^{-2} s^{-1} (without filter), X_{PCE} = 99.93%; (b) volumetric flow rate = 4.17 cm^3 s^{-1}, C^{in}_{PCE} = 50 mg m^{-3}, relative humidity = 48%, SRPA = 1.0×10^{-11} Einstein cm^{-2} s^{-1}, X_{PCE} = 40.55%. *Keys*: (—) $z = 0$, (- - -) $z = \frac{1}{3}\ Z_R$, (· · ·) $z = \frac{2}{3}\ Z_R$, (· · · · ·) $z = Z_R$.; (c) dimensionless radial velocity profiles.

UNCORRECTED PROOF

Please cite this article as: G.Imoberdorf, E., et al., Simulation of a multi-annular photocatalytic reactor for degradation of perchloroethylene in air. Chemical Engineering Science (2006), doi: 10.1016/j.ces.2006.10.024

Because the PCE concentration was kept at very low levels in all the experimental runs (i.e., lower than $50\,\mathrm{mg\,m^{-3}}$), the velocity profile of the gas phase in each annular section is, for all practical purposes, independent of both the reaction rate and the mass transfer rate. Therefore, the velocity field can be computed directly from Eq. (1). The mathematical problem comprising the differential mass balance equation (Eq. (2)), together with the boundary conditions of Eqs.(3)–(7), was numerically solved using a method of finite differences. Finally, the outlet PCE concentration was calculated from the discrete PCE concentration profiles at the reactor output stream (Eq. (8)).

Experimental and predicted PCE concentrations at the reactor outlet are compared in Fig. 6. The agreement is satisfactory over the entire range of the operating conditions, whose details have been reported elsewhere (Imoberdorf et al., 2006). Predicted PCE conversions compared with experimental results show a root mean square error less than 5.6%. These results should be regarded as a validation of the simulation model, thus opening the possibility to its use as a very useful tool in predicting the impact of different sets of operating conditions and design parameters on the reactor performance.

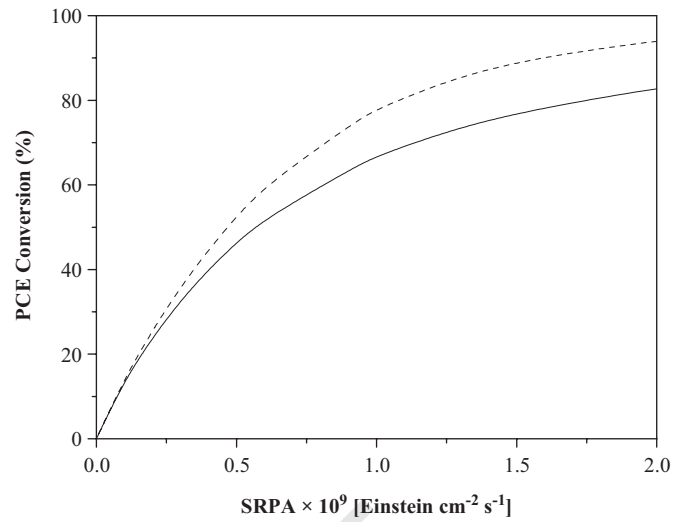

Fig. 8. Predictions of PCE conversion for different SRPA levels (volumetric flow rate $=150\,\mathrm{cm^3\,s^{-1}}$, relative (humidity $=48\%$, $C^{\mathrm{in}}_{\mathrm{PCE}}=50\,\mathrm{mg\,m^{-3}}$). *Keys*: (—) complete model, (· · ··) reference model.

6. Parametric analysis

6.1. PCE radial concentration profiles

The simulation program validated in the previous section against experimental results contains the essentials of the photoreactor "physiology". Therefore, within the validity limits of its tributary models (mainly, the reaction rate expression) the simulation program can be used to predict the reactor behavior under operating conditions different than those adopted for the experimental runs. Moreover, it can produce a description of the relative impact of different concurrent phenomena at a level of detail frequently beyond experimental possibilities. In this section, we will study the reactor performance under two well differentiated situations, such as those of high and low irradiation levels. Of particular interest will be to identify the conditions and the reactor zones where the onset of PCE concentration gradients may occur. This is so because of the negative impact that concentration gradients have on the reactor energy performance.

In Fig. 7, dimensionless concentration profiles from simulation runs are shown (Figs. 7a–b), as well as the corresponding dimensionless velocity profiles (Fig. 7c). The results of Fig. 7a were obtained adopting a volumetric flow rate of $30\,\mathrm{cm^3\,s^{-1}}$, at full irradiation conditions (i.e., without attenuating the intensity of the radiation beams emitted by the lamp), with a $\mathrm{SRPA}=1.56\times10^{-9}\,\mathrm{Einstein\,cm^{-2}\,s^{-1}}$. On the other hand, the results of Fig. 7b correspond to a flow rate of $4.17\,\mathrm{cm^3\,s^{-1}}$ and an irradiation level attenuated by neutral filters down to a value of the $\mathrm{SRPA}=1.0\times10^{-11}\,\mathrm{Einstein\,cm^{-2}\,s^{-1}}$.

As shown in Fig. 7a, when the full lamp output power is used and the gas volumetric flow rate is $30\,\mathrm{cm^3\,s^{-1}}$, the PCE conversion at the exit of the outer annulus is 28.74%. Under the same conditions, the PCE conversion at the exit of the intermediate annulus is 84.79% and reaches 99.93% at the reactor outlet. From the results of Fig. 7a, it can be also seen that there are no appreciable PCE concentration radial gradients in the feed (outer) annulus. This means that PCE flows through this annular duct with an almost uniform concentration radial profile, superimposed to the quasi-parabolic velocity profile of the background laminar airflow, which is shown in Fig. 7c. This is no longer true for the inner annulus due to the existence of faster reaction rates caused by higher LSRPA values. Here, the reaction rate begins to compete against the molecular diffusion of PCE from the bulk to the catalytic walls and radial gradients clearly start building up. Moreover, due to the higher reaction rates occurring in this (inner) annulus, the PCE concentration diminishes more rapidly along the axial direction than it does in the other two annuli. The evident asymmetry of the PCE profile in this annulus is a consequence of the different reaction rate values resulting from different LSRPA existing on the inner and outer TiO_2 photocatalytic surfaces in contact with the flowing gas phase (Fig. 5).

From the results shown in Fig. 7b, it can be seen that the PCE conversion at the exit of the outer annulus is 1.61%, while at the exit of the intermediate annulus is 9.14%, and 40.56% at the reactor outlet. Due to the low reaction rates, there are no appreciable PCE concentration radial gradients (i.e., the photocatalytic reaction is the rate controlling step of the overall diffusion-with-chemical-reaction process).

In Fig. 8, the predicted PCE conversions vs. the SRPA, alternatively using the complete (Eqs. (2)–(8)) and the reference models (Eq. (28)), are shown. Both models predict the same values of PCE conversions at low SRPA. In such conditions, the reference model could be applied to predict the PCE conversion. On the other hand, for high values of SRPA, significant deviations can be observed. For these cases, the reference model can not be applied.

UNCORRECTED PROOF

Please cite this article as: G.Imoberdorf, E., et al., Simulation of a multi-annular photocatalytic reactor for degradation of perchloroethylene in air. Chemical Engineering Science (2006), doi: 10.1016/j.ces.2006.10.024

Table 2
Radiative energy efficiencies for the multi-annular photocatalytic reactor

Radiative energy efficiency	Values (%)
η_I	83
η_A	92
η_R	<2.5
η_{app}	<2.3
η_T	<1.9

7. Radiative energy efficiencies

For a given reactor and a non-participative fluid phase, the efficiencies η_I and η_A are constant. In the case of the multi-annular photocatalytic reactor, their values were obtained from Eqs. (21) and (22), respectively. The spectral net radiation flux on the reactor wall of radiation entrance (directly exposed to the lamp irradiation), $q_{\lambda,RW}$, has been computed from Eqs. (14) and (15), using the spectral emission power of the lamp ($P_{\lambda,L}$). The values of the LSRPA on the thin TiO_2 catalytic films were computed from Eq. (17). Numerical values of η_R were calculated using the complete model (Eqs. (2)–(8) and Eq. (24)) under different operating conditions. Values of η_I, η_A and η_R obtained in this way are shown in Table 2, as well as those of η_{app}. These results show that photons are efficiently transmitted from the source to the reactor, as can be concluded from the high η_I value. Also the high value obtained for η_A reveals that once photons enter the reactor, they are efficiently absorbed by the catalytic films. The relatively low values obtained for η_R ($<2.5\%$) are caused by the low PCE concentrations used. A correct interpretation of the η_R values requires of an especial analysis of its functional dependence on the different operating variables, which is intended in what follows.

Although the values of η_{app} obtained in this work are much lower than those reported by other authors (see the Introduction section), the reactor performances are comparable when the linear dependence of the overall reaction quantum efficiency on the PCE concentration is considered. In our case, the smaller values of the apparent quantum efficiency is a direct consequence of the fact that we used smaller PCE concentrations.

Computed results of η_R as a function of the gas flow rate is shown in Fig. 9a, for low irradiation levels (1.0×10^{-11} Einstein cm^{-2} s^{-1}). While η_R increases with increasing flow rates, the PCE conversion decreases. In the region of low gas flow rates the PCE conversion may reach values close to 100%, but at the same time η_R falls dramatically. According to Eq. (26), this is the direct consequence of the functional dependence of $\eta_{R,\text{loc}}$ on the PCE local concentration. The same effect, but from a different standpoint, can be observed in Fig. 9b, where it is shown that the PCE conversion increases and η_R decreases with increasing values of the SRPA.

Fig. 10 shows the variation of η_R with PCE conversion for two irradiation levels: at low irradiation level where the value of the SRPA is 1.0×10^{-10} Einstein cm^{-2} s^{-1}, and at high irradiation level where the value of the SRPA is 1.0×10^{-9} Einstein cm^{-2} s^{-1}. The dotted lines correspond to the results of $\eta_{R,\text{ref}}$, which were obtained with Eq. (30). This amounts to disregard radial concentration gradients and therefore, absence of mass transfer control. As may be seen in Eq. (26), $\eta_{R,\text{loc}}$ for the considered reaction does not depend on the LSRPA, and it only depends on the values of the PCE concentration as well as the local relative humidity. This result would have been different if the reaction kinetics had a different dependence with respect to the LSRPA. In the absence of concentration radial gradients, η_R obtained with the complete model coincides with the one obtained using the simplified reference model, just as it happens for low values of the SRPA. The observed discrepancies for high values of the SRPA are due to the formation of PCE concentration gradients as a consequence of the resulting higher superficial rates of reaction. For conversions of 50% η_R drops from 0.93% to 0.69% for low and high SRPA values, respectively.

It is worth to stress the strong dependence of η_R on the reactor outlet conversion. It varies from 1.28% for conversions close

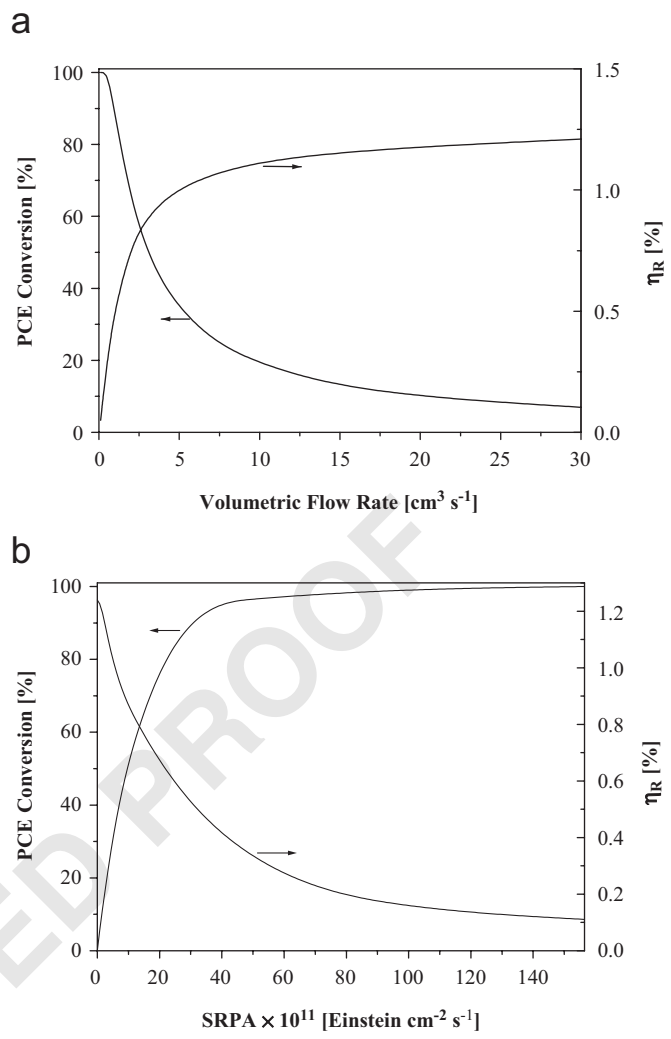

Fig. 9. PCE conversion and overall reaction quantum efficiency for different values of: (a) volumetric flow rates (SRPA $= 1.0 \times 10^{-11}$ Einstein cm^{-2} s^{-1}, relative humidity=48%, $C^{\text{in}}_{\text{PCE}}$=50 mg m^{-3}) and (b) SRPA values (volumetric flow rate = 30 cm^3 s^{-1}, relative humidity = 48%, $C^{\text{in}}_{\text{PCE}}$ = 50 mg m^{-3}).

UNCORRECTED PROOF

Please cite this article as: G.Imoberdorf, E., et al., Simulation of a multi-annular photocatalytic reactor for degradation of perchloroethylene in air. Chemical Engineering Science (2006), doi: 10.1016/j.ces.2006.10.024

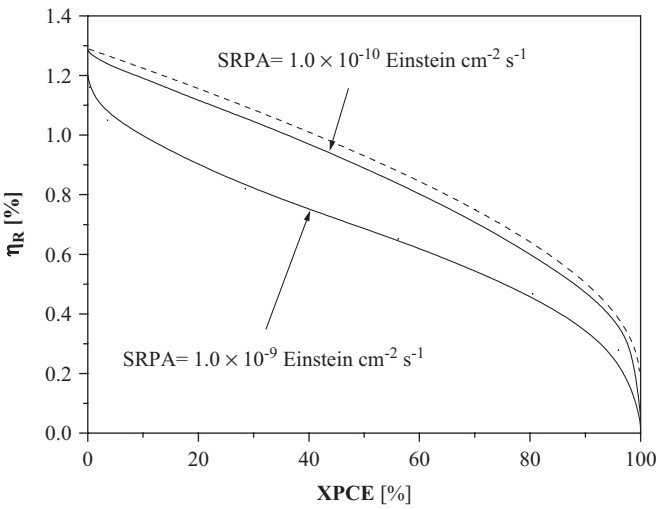

Fig. 10. Overall reaction quantum efficiency as a function of PCE conversion for two radiation levels.

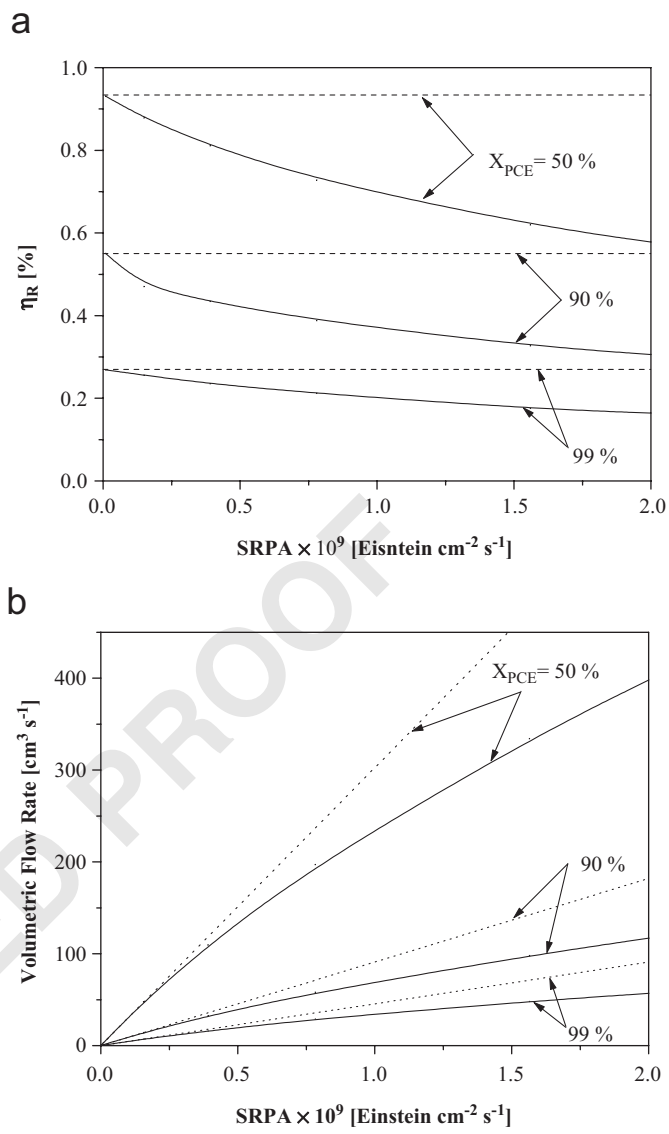

Fig. 11. (a) Overall reaction quantum efficiency as a function of SPRA values for 50%, 90% and 99% PCE conversions (relative humidity = 46%) and (b) corresponding volumetric flow rates.

to zero, to 0% for conversions near 100%. Note that the values of η_R in this range are predicted always using the same multi-annular reactor and the same contaminant initial concentration. The rest of the parameters, such as the relative humidity and the irradiation level also remained constant. Therefore, it is important to analyse the effect of these operating variables on η_R, for fixed values of the outlet conversion.

In Fig. 11a, values of η_R are shown for different values of the SRPA and different conversions, at constant PCE initial concentration (50 mg m^{-3}) and constant relative humidity (48%). Fig. 11b is complementary to Fig. 11a, since it shows the gas volumetric flow rates corresponding to the operating conditions of Fig. 11a. The dotted lines in Figs. 11a, b represent the results predicted with the simplified reference model (Eqs. (30) and (28)). By comparison with the full lines, representing the results obtained with the complete model, the effect of the occurrence of radial gradients in the reactor channels becomes apparent. Note that η_R diminishes with increasing the SRPA levels. The reaction rate increases and mass transport phenomena progressively dominate the overall mass transfer-chemical reaction rate process. As a consequence of this, radial PCE concentration gradients become increasingly important (Fig. 7a). In the case of large SRPA values (around 2.0×10^{-9} Einstein cm^{-2} s^{-1}), the η_R value plunges down to 40% of the reference value, $\eta_{R,\mathrm{ref}}$. However, the increase of the SRPA value allows to step up the volumetric flow rate at the chosen constant PCE conversion (Fig. 11b).

The results obtained suggest that the performance of the multi-annular reactor would be improved by varying the thickness of the photocatalytic films as a function of their distance from the lamp, so that a more uniform distribution of the LSRPA in the reactor can be achieved. Thinner films would have to be deposited on the walls of the inner tubes, where the energy flux is larger than on the outer tubes, thus lowering the concentration gradients by slowing down the reaction rates. On the other hand, thicker films would have to be deposited on the walls of the outer tubes, in order to maximize the η_A values, as long as we keep the film thickness at lower values than those for which internal diffusive resistances may become important. From modeling results (assuming volumetric flow rate = 100 cm^3 s^{-1}, $C^{\mathrm{in}}_{\mathrm{PCE}}$ = 50 mg m^{-3}, relative humidity = 48%, SRPA = 1.56×10^{-9} Einstein cm^{-2} s^{-1}) the predicted PCE conversion of the original multi-annular reactor (uniform thickness of all the TiO_2 films) is equal to 89.7%, but the predicted PCE conversion of the modified multi-annular reactor (uniform distribution of the LSRPA in all the TiO_2 films) is increased to 94.2%. A further analysis of the optimization possibilities and improvements in the configuration of the multi-annular reactor will be discussed in a forthcoming publication.

The predicted effect of the relative humidity on η_R is shown in Fig. 12. Regardless of the outlet conversion value chosen for the analysis, both the η_R and the reactor processing capacity

UNCORRECTED PROOF

Please cite this article as: G.Imoberdorf, E., et al., Simulation of a multi-annular photocatalytic reactor for degradation of perchloroethylene in air. Chemical Engineering Science (2006), doi: 10.1016/j.ces.2006.10.024

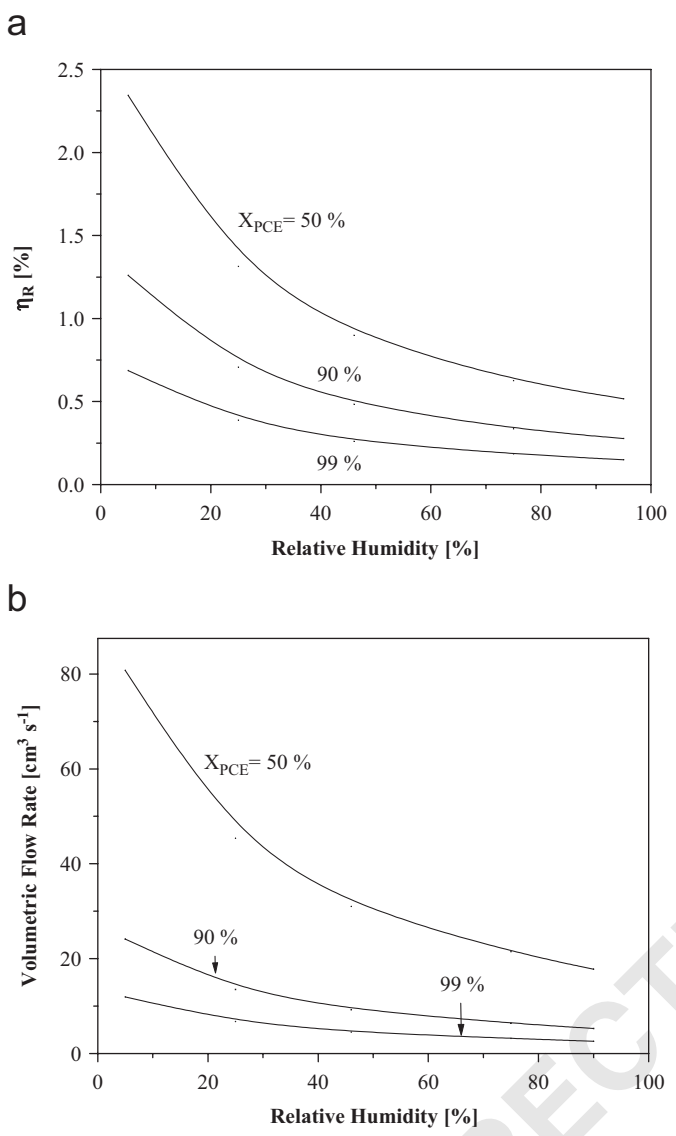

Fig. 12. (a) Overall reaction quantum efficiency as a function of relative humidity for 50%, 90% and 99% PCE conversions (SRPA $= 1.0 \times 10^{-10}$ Einstein cm^{-2} s^{-1}) and (b) corresponding volumetric flow rates.

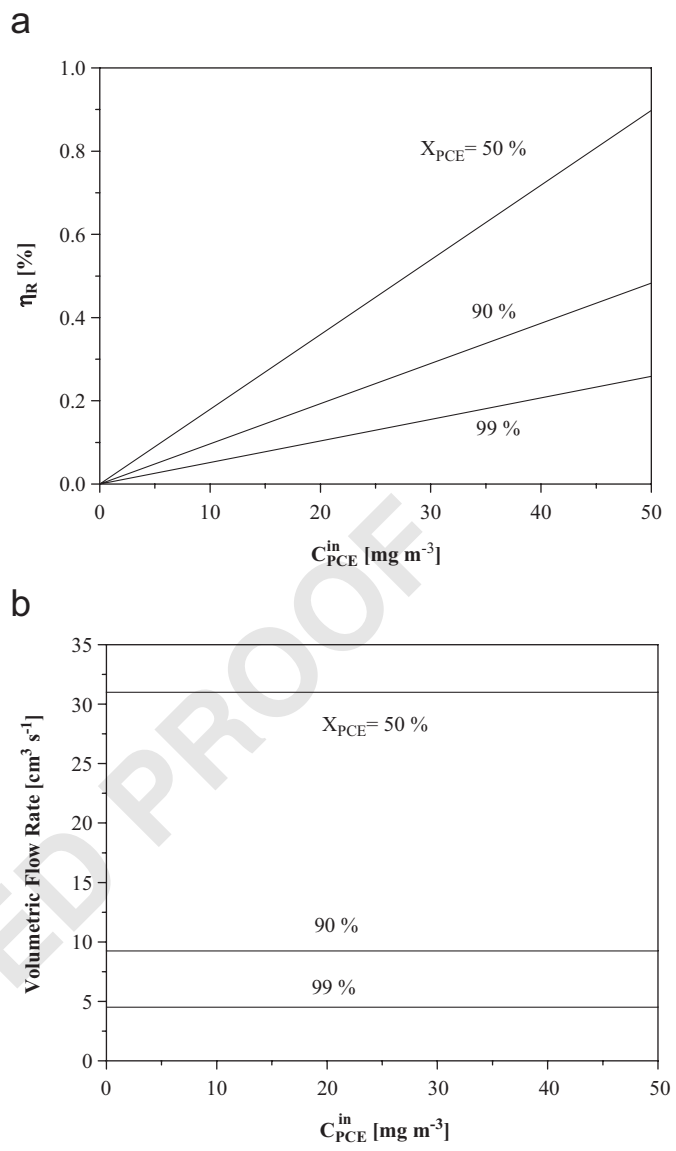

Fig. 13. (a) Overall reaction quantum efficiency as a function of PCE inlet concentration for 50%, 90% and 99% PCE conversions (relative humidity = 46%, SRPA $= 1.0 \times 10^{-10}$ Einstein cm^{-2} s^{-1}) and (b) corresponding volumetric flow rates.

UNCORRECTED PROOF

(proportional to the contaminated stream flow rate) diminish to one-fifth of the initial value when the relative humidity changes from 5% to 95%. An explanation of the effect of humidity on the reaction rate can be approached from different directions. On one hand, there is full agreement between different authors for the TCE photocatalytic degradation (Wang et al., 1998; Amama et al., 2001) in that the water and the TCE compete for the same adsorption sites. As a result of this, increasing the concentration of water in the gas phase diminishes the amount of adsorbed TCE. In addition to the competitive adsorption, according to Amama et al. (2001) water molecules in the gas phase may suppress the chain propagation of the chlorine radical.

In Fig. 13 the predicted effect of the initial PCE concentration on η_R is shown. The efficiency η_R is proportional to the PCE feed concentration, not only for low SRPA values, but also for those large enough to give rise to important PCE concentration gradients. Note that the flow rates of contaminated air that can be processed diminish with conversion, ranging from 31 cm^3 s^{-1} for a conversion of 50% to 4.5 cm^3 s^{-1} for a conversion of 99%.

8. Conclusions

A multi-annular photocatalytic reactor was designed, that shows good effectiveness for perchloroethylene (PCE) removal from contaminated air streams. A previously developed physical and mathematical model for the multi-annular concentric photoreactor was used to study the radiative energy efficiency of this reactor. This analysis was made in a way that accounts for the impact on the total radiative energy efficiency of each

Please cite this article as: G.Imoberdorf, E., et al., Simulation of a multi-annular photocatalytic reactor for degradation of perchloroethylene in air. Chemical Engineering Science (2006), doi: 10.1016/j.ces.2006.10.024

event in the succession starting with the initial emission of photons by the lamp and ending with their final usage in the catalytic degradation reaction.

For the multi-annular reactor described before, the radiation incidence efficiency was 83%, and the catalyst radiation absorption efficiency was 92%, values that are function of the reactor-UV lamp characteristics, but do not depend on the particular reaction or the operating conditions.

The overall reaction quantum efficiency (η_R) for PCE degradation depends upon operating variables of the multi-annular photocatalytic reactor, such as the PCE feed concentration and conversion, gas flow rate, irradiation level, relative air humidity, and mass transfer limitations. Under the operating conditions used in this work, the obtained values of η_R were lower than 2.5%.

The η_R shows a monotonic dependence upon the local PCE concentration, increasing with increasing pollutant concentrations. Related with this effect, the η_R dramatically decreases when the PCE conversion increases (with values close to 0% for PCE conversions near 100%). As a consequence of this, achieving large PCE outlet conversions requires working at low values of η_R. Regardless of the outlet conversion value chosen for the analysis, both the η_R and the reactor processing capacity diminish when the relative humidity increases.

At low irradiation levels ($< 1.0 \times 10^{-10}$ Einstein cm^{-2} s^{-1}) the reactor performance is kinetically controlled and mass transfer phenomena are not the determining rate step. Under these operating conditions, PCE radial concentration gradients are negligible. At higher irradiation levels ($> 1.5 \times 10^{-9}$ Einstein cm^{-2} s^{-1}), molecular diffusion of PCE from the bulk to the catalytic walls begins to control and noticeable radial gradients start to build up.

Finally, it should be stressed that the radiation incidence efficiency (η_I) and the catalyst radiation absorption efficiency (η_A) may be used to compare the photon capture ability of various types of photocatalytic reactor configurations for pollution remediation (annular, monolith, flat plate, optical fibers, etc.), even if these reactors are operated under different operating conditions and with different chemical pollutants. On the other hand, under negligible mass transfer resistances, η_R does not depend on the photocatalytic reactor configuration. This parameter is useful to compare the catalytic activity of different catalysts for the same pollutant or of the same photocatalyst for different pollutants.

Notation

A	area, cm^2
C	mass concentration, mg m^{-3}
D^0	molecular diffusivity, cm^2 s^{-1}
e	thickness, cm
$e^{a,s}$	local superficial rate of photon absorption, Einstein s^{-1} cm^{-2}
I	specific radiation intensity, Einstein s^{-1} cm^{-2} sr^{-1}
k	kinetic parameter, units depend on the reaction step
K	equilibrium constant, m^3 mg^{-1}
n	number of times that a radiation beam has been attenuated by each media, dimensionless
$\underline{n}_G$	outwardly directed unit normal to the catalytic film, dimensionless
P	emission power, W or Einstein s^{-1}
q	local net radiation flux, Einstein s^{-1} cm^{-2}
Q	volumetric flow rate, cm^3 s^{-1}
r	reaction rate, mol cm^{-2} s^{-1}; also radial coordinate, cm
R	radius, cm
V_z	axial velocity, cm s^{-1}
X	conversion, dimensionless
z	axial coordinate, cm
Z	length, cm

Greek letters

α	kinetic parameter, m^3 Einstein^{-1}
γ	cylindrical coordinate, rad
η	quantum efficiency, dimensionless
θ	spherical coordinate, rad
κ	volumetric absorption coefficient, cm^{-1}
λ	wavelength, nm
ϕ	spherical coordinate, rad
χ	internal/external radius ratio, dimensionless

Subscripts

λ	denotes wavelength
A	relative to absorption of radiation
Air	relative to air
app	apparent
C	relative to cross-sectional area
f	relative to the TiO_2 film
g	relative to the electron-hole generation step; also relative to glass
H_2O	relative to water
I	relative to the incident radiation
j	relative to the annular section (1 = inner, 2 = intermediate, 3 = outer)
L	relative to the UV lamp
loc	local
M	relative to the element that participates in the radical inactivation
max	relative to the maximum limiting value
min	relative to the minimum limiting value
n	normal to the reaction area of the photocatalytic surface
PCE	relative to perchloroethylene
R	relative to the reaction; also relative to reactor
ref	relative to the reference model
RW	relative to the reactor wall of radiation entrance
T	relative to the total radiation

Superscripts

i	relative to the incident radiation flux
in	relative to the inlet stream

UNCORRECTED PROOF

Please cite this article as: G.Imoberdorf, E., et al., Simulation of a multi-annular photocatalytic reactor for degradation of perchloroethylene in air. Chemical Engineering Science (2006), doi: 10.1016/j.ces.2006.10.024

out	relative to the outlet stream
t	related to the transmitted radiation flux

Special symbols

$\langle\cdot\rangle$	means average value over a defined space

Acknowledgments

The authors are grateful to Universidad Nacional del Litoral (UNL), Consejo Nacional de Investigaciones Científicas y Técnicas (CONICET) and Agencia Nacional de Promoción Científica y Tecnológica (ANPCyT) for financial support. Thanks are also given to Eng. Gerardo Rintoul for his participation in some parts of the experimental work.

Appendix A

By integration of the differential mass balance Eq. (2) in the cross-sectional area

$$\int_{r=\chi_j R_j}^{R_j}\int_{\gamma=0}^{2\pi}\frac{\partial C_{\mathrm{PCE}}(r,z)}{\partial z}V_{z,j}(r)r\,\mathrm{d}\gamma\,\mathrm{d}r = \int_{r=\chi_j R_j}^{R_j}\int_{\gamma=0}^{2\pi}D^0_{\text{PCE-Air}}\frac{\partial}{\partial r}\times\left(r\frac{\partial C_{\mathrm{PCE}}(r,z)}{\partial r}\right)\mathrm{d}\gamma\,\mathrm{d}r \quad (j=1,2,3). \tag{A.1}$$

Eq. (A.1) may be expressed as

$$\frac{\partial}{\partial z}\int_{r=\chi_j R_j}^{R_j}\int_{\gamma=0}^{2\pi}C_{\mathrm{PCE}}(r,z)V_{z,j}(r)r\,\mathrm{d}\gamma\,\mathrm{d}r = 2\pi D^0_{\text{PCE-Air}}R_j\left.\frac{\partial C_{\mathrm{PCE}}(r,z)}{\partial r}\right|_{R_j} - 2\pi\, D^0_{\text{PCE-Air}}\chi_j R_j\left.\frac{\partial C_{\mathrm{PCE}}(r,z)}{\partial r}\right|_{\chi_j R_j}. \tag{A.2}$$

From the boundary conditions of Eqs. (3) and (4)

$$\frac{\partial}{\partial z}\int_{r=\chi_j R_j}^{R_j}\int_{\gamma=0}^{2\pi}C_{\mathrm{PCE}}(r,z)V_{z,j}(r)r\,\mathrm{d}\gamma\,\mathrm{d}r = 2\pi R_j r_{\mathrm{PCE}}(R_j,z) + 2\pi\chi_j R_j r_{\mathrm{PCE}}(\chi_j R_j,z). \tag{A.3}$$

The PCE average concentration value in the cross-sectional area is defined as

$$\langle C_{\mathrm{PCE}}\rangle_{A_{C_j}}(z) = \frac{\int_{r=\chi_j R_j}^{R_j}\int_{\gamma=0}^{2\pi}C_{\mathrm{PCE}}(r,z)V_{z,j}(r)r\,\mathrm{d}\gamma\,\mathrm{d}r}{\int_{r=\chi_j R_j}^{R_j}\int_{\gamma=0}^{2\pi}V_{z,j}(r)r\,\mathrm{d}\gamma\,\mathrm{d}r} = \frac{(-1)^{j+1}}{Q}\int_{r=\chi_j R_j}^{R_j}\int_{\gamma=0}^{2\pi}C_{\mathrm{PCE}}(r,z)V_{z,j}(r)r\,\mathrm{d}\gamma\,\mathrm{d}r. \tag{A.4}$$

Substitution of Eq. (A.4) and the kinetic expression (Eq. (10)) in Eq. (A.3)

$$\frac{\partial}{\partial z}\left(\langle C_{\mathrm{PCE}}\rangle_{A_{C_i}}(z)(-1)^{j+1}Q\right) = 2\pi R_j\frac{\alpha C_{\mathrm{PCE}}(r,z)}{1+K_{\mathrm{H_2O}}C_{\mathrm{H_2O}}}e^{a,s}(R_j,z) + 2\pi\chi_j R_j\frac{\alpha C_{\mathrm{PCE}}(r,z)}{1+K_{\mathrm{H_2O}}C_{\mathrm{H_2O}}}e^{a,s}(\chi_j R_j,z). \tag{A.5}$$

For negligible PCE radial concentration gradients, the following simplification can be assumed

$$C_{\mathrm{PCE}}(r,z)\cong\langle C_{\mathrm{PCE}}\rangle_{A_{C_i}}(z). \tag{A.6}$$

With this assumption, Eq. (A.5) may be written as

$$(-1)^{j+1}Q\frac{\partial}{\partial z}\langle C_{\mathrm{PCE}}\rangle_{A_{C_i}}(z) = 2\pi R_j\frac{\alpha\langle C_{\mathrm{PCE}}\rangle_{A_{C_i}}(z)}{1+K_{\mathrm{H_2O}}C_{\mathrm{H_2O}}}e^{a,s}(R_j,z) + 2\pi\chi_j R_j\frac{\alpha\langle C_{\mathrm{PCE}}\rangle_{A_{C_i}}(z)}{1+K_{\mathrm{H_2O}}C_{\mathrm{H_2O}}}e^{a,s}(\chi_j R_j,z). \tag{A.7}$$

By integration of Eq. (A.7)

$$\frac{\langle C_{\mathrm{PCE}}\rangle_{A_{C_j}}(Z_R)}{\langle C_{\mathrm{PCE}}\rangle_{A_{Cj}}(0)} = \exp\left(-\frac{2\pi\alpha}{Q(1+K_{\mathrm{H_2O}}C_{\mathrm{H_2O}})}\times\left(\chi_1 R_1\int_{z=0}^{Z_R}e^{a,s}(\chi_j R_j,z)\,\mathrm{d}z + R_j\int_{z=0}^{Z_R}e^{a,s}(R_j,z)\,\mathrm{d}z\right)\right). \tag{A.8}$$

Besides, the boundary conditions expressed in Eqs. (5)–(8), are given by

$$\langle C_{\mathrm{PCE}}\rangle_{A_{C_3}}(0)=C^{\mathrm{in}}_{\mathrm{PCE}},\quad \langle C_{\mathrm{PCE}}\rangle_{A_{C_3}}(Z_R)=\langle C_{\mathrm{PCE}}\rangle_{A_{C_2}}(Z_R),$$
$$\langle C_{\mathrm{PCE}}\rangle_{A_{C_2}}(0)=\langle C_{\mathrm{PCE}}\rangle_{A_{C_1}}(0),\quad \langle C_{\mathrm{PCE}}\rangle_{A_{C_1}}(Z_R)=C^{\mathrm{out}}_{\mathrm{PCE}}. \tag{A.9}$$

Replacing Eqs. (A.9) and the SRPA Eq. (19) into Eq. (A.8)

$$\frac{C^{\mathrm{out}}_{\mathrm{PCE}}}{C^{\mathrm{in}}_{\mathrm{PCE}}} = \exp\left(-\frac{\alpha A_R\langle e^{a,s}\rangle_{A_R}}{Q(1+K_{\mathrm{H_2O}}C_{\mathrm{H_2O}})}\right). \tag{A.10}$$

Finally, the PCE conversion is given by

$$X_{\mathrm{PCE}} = \frac{C^{\mathrm{in}}_{\mathrm{PCE}}-C^{\mathrm{out}}_{\mathrm{PCE}}}{C^{\mathrm{in}}_{\mathrm{PCE}}} = 1-\frac{C^{\mathrm{out}}_{\mathrm{PCE}}}{C^{\mathrm{in}}_{\mathrm{PCE}}} = 1-\exp\left(-\frac{\alpha A_R\langle e^{a,s}\rangle_{A_R}}{Q(1+K_{\mathrm{H_2O}}C_{\mathrm{H_2O}})}\right). \tag{A.11}$$

References

Amama, P.B., Itoh, K., Murabayashi, M., 2001. Photocatalytic oxidation of trichloroethylene in humidified atmosphere. Journal of Molecular Catalysis A: Chemical 176, 165–172.

UNCORRECTED PROOF

Please cite this article as: G.Imoberdorf, E., et al., Simulation of a multi-annular photocatalytic reactor for degradation of perchloroethylene in air. Chemical Engineering Science (2006), doi: 10.1016/j.ces.2006.10.024

Blake, D.M., 2001. Bibliography of work on the heterogeneous photocatalytic removal of hazardous compounds from water and air 2001. National Renewable Energy Laboratory, Golden, Colorado.

Braun, A.M., Maurette, M.T., Oliveros E., 1986. In: Braunsarl (Ed.), Technologie Photochimique. Culture-Factory, Paris, France. ISBN: 2-88074-095-9.

Buechler, K.J., Noble, R.D., Koval, C.A., Jacoby, W.A., 1999. Investigation of the effects of controlled periodic illumination on the oxidation of gaseous trichloroethylene using a thin film of TiO_2. Industrial & Engineering Chemical Research 38, 892–896.

Cabrera, M.I., Alfano, O.M., Cassano, A.E., 1994. Novel reactor for photocatalytic kinetic studies. Industrial & Engineering Chemistry Research 33, 3031–3042.

Cassano, A.E., Martín, C.A., Brandi, R.J., Alfano, O.M., 1995. Photoreactor analysis and design: fundamentals and applications. Industrial & Engineering Chemical Research 34, 2155–2201.

Cerdá, J., Marchetti, J.L., Cassano, A.E., 1977. Radiation efficiencies in elliptical photoreactors. Latin American Journal of Heat and Mass Transfer 1, 33–63.

Demeestere, K., de Visscher, A., Dewulf, J., Van Leeuwen, M., Van Langenhove, H., 2004. A new kinetic model for titanium dioxide mediated heterogeneous photocatalytic degradation of trichloroethylene in gas-phase. Applied Catalysis B: Environmental 54, 261–274.

Fujishima, A., Rao, T.N., Tryk, D.A., 2000. Titanium dioxide photocatalysis. Journal of Photochemistry and Photobiology C: Photochemistry Reviews 1, 1–21.

Hegedüs, M., Dombi, A., 2004a. Gas-phase heterogeneous photocatalytic oxidation of chlorinated ethenes over titanium dioxide: perchloroethene. Applied Catalysis B: Environmental 53, 141–151.

Hegedüs, M., Dombi, A., 2004b. Gas-phase heterogeneous photocatalytic oxidation of chlorinated ethenes over titanium dioxide: perchloroethene. Applied Catalysis B: Environmental 53, 141–151.

Hoffman, M.R., Martin, S.T., Choi, W., Bahnemann, D.W., 1995. Environmental applications of semiconductor photocatalysis. Chemical Review 95, 69–96.

Hossain, M.M., Raupp, G.B., 1999. Polychromatic radiation field model for a honeycomb monolith photocatalytic reactor. Chemical Engineering Science 54, 3027–3034.

Hung, C.H., Mariñas, B.J., 1997. Role of water in the photocatalytic degradation of trichloroethylene vapor on TiO_2 films. Environmental Science Technology 31, 1440–1445.

Ibrahim, H., de Lasa, H., 2003. Photo-catalytic degradation of air borne pollutants. Apparent quantum efficiencies in a novel photo-CREC-air reactor. Chemical Engineering Science 58, 943–949.

Imoberdorf, G.E., Irazoqui, H.A., Cassano, A.E., Alfano, O.M., 2005. Photocatalytic degradation of tetrachloroethylene in gas phase on TiO_2 films: a kinetic study. Industrial Engineering Chemical Research 44, 6075–6085.

Imoberdorf, G.E., Cassano, A.E., Alfano, O.M., Irazoqui, H.A., 2006. Modeling of a multi-annular photocatalytic reactor for tetrachloroethylene degradation in moist air. A.I.Ch.E. Journal, in press.

Jacoby, W.A., Blake, D.M., Noble, R.D., Koval, C.A., 1995. Kinetics of the oxidation of trichloroethylene in air via heterogeneous photocatalysis. Journal of Catalysis 157, 87–96.

Li, G.H., An, W.Z., 2000. A proposed mechanism of photocatalytic oxidation of trichloroethylene in gas phase. Chinese Chemical Letters 11, 31–34.

Peral, J., Domènech, X., Ollis, D.F., 1997. Heterogeneous photocatalysis for purification, decontamination and deodorization of air. Journal of Technology and Biotechnology 70, 117–140.

Raupp, G.B., Alexiadis, A., Hossain, M., Changrani, R., 2001. First-principles modeling, scaling laws and design of structured photocatalytic oxidation reactors for air purification. Catalysis Today 69, 41–49.

Sanhueza, E., Hisatsune, I.C., Heiklen, J., 1976. Oxidation of haloethylenes. Chemical Review 76, 801–826.

Serpone, N., Emeline, A.V., 2002. Suggested terms and definitions in photocatalysis and radiocatalysis. International Journal of Photoenergy 4, 91–131.

Tanimura, T., Yoshida, A., Yamazaki, S., 2005. Reduced formation of undesirable by-products from photocatalytic degradation of trichloroethylene. Applied Catalysis B: Environmental 61, 346–351.

Wang, K., Tsai, H.H., Hsieh, Y.H., 1998. The kinetic of the degradation of trichloroethylene in gas phase over TiO_2 supported on glass bead. Applied Catalysis B: Environmental 17, 313–320.

Wang, K.H., Jehng, J.M., Hsieh, Y.H., Chang, C.Y., 2002. The reaction pathway for the heterogeneous photocatalysis of trichloroethylene in gas phase. Journal of Hazardous Materials B90, 63–75.

Yamazaki, S., Araki, K., 2002. Photocatalytic degradation of tri- and tetrachloroethylene on porous TiO_2 pellets. Electrochemistry 70, 412–415.

Yamazaki, S., Tsukamoto, H., Araki, K., Tanimura, T., Tejedor-Tejedor, I., Anderson, M.A., 2001. Photocatalytic degradation of gaseous tetrachloroethylene on porous TiO_2 pellets. Applied Catalysis B: Environmental 33, 109–117.

Yamazaki, S., Tanimura, T., Yoshida, A., 2004. Reaction mechanism of photocatalytic degradation of chlorinated ethylenes on porous TiO_2 pellets: Cl radical-initiated mechanism. Journal of Physical Chemistry A 108, 5183–5188.

Yamazaki–Nishida, S., Nagano, K.J., Phillips, L.A., Cervera-March, S., Anderson, M.A., 1993. Photocatalytic degradation of trichloroethylene in the gas phase using TiO_2 pellets. Journal of Photochemical and Photobiology A: Chemical 70, 95–99.

Zhao, L., Ozaki, S., Itoh, K., Murabayashi, M., 2002. Self-catalytic behavior in gas-phase photocatalytic oxidation of trichloroethylene using TiO_2. Electrochemistry 70, 8–12.

UNCORRECTED PROOF

Please cite this article as: G.Imoberdorf, E., et al., Simulation of a multi-annular photocatalytic reactor for degradation of perchloroethylene in air. Chemical Engineering Science (2006), doi: 10.1016/j.ces.2006.10.024